

# Synthesis and characterization of a new fluorescent probe for reactive oxygen species†

Belinda Heyne, Chad Beddie and J. C. Scaiano\*

Received 19th February 2007, Accepted 12th March 2007

First published as an Advance Article on the web 2nd April 2007

DOI: 10.1039/b702618h

We report the development of a new fluorescence sensor for reactive oxygen species (ROS) based on a benzofurazan structure. The sensor, NBFhd, is initially non-fluorescent and reacts with peroxy radicals by hydrogen transfer in an aqueous medium under neutral conditions to release the fluorescent *N*-methyl-4-amino-7-nitrobenzofurazan (NBF) and 1,4-benzoquinone. NBFhd shows excellent contrast and no interference in the region of cell autofluorescence and is a new tool to detect ROS in homogeneous and biological systems.

## Introduction

Reactive oxygen species (ROS) formed during the metabolism of oxygen are believed to be implicated in aging processes and numerous diseases such as atherosclerosis and cancer.<sup>1–6</sup> Recently, in order to gain insight into the exact implication of ROS in different physiopathologies, research has focused on the characterization of new sensors able to detect ROS in organisms.<sup>7–11</sup>

Because of its non-invasive character and its high sensitivity, fluorescence is frequently the preferred technique to detect ROS *in vitro* as well as *in vivo*. Several fluorescence sensors have been developed for this purpose; among them, 2-[6-(4'-hydroxy)phenoxy-3H-xanthen-3-on-9-yl] benzoic acid (HPF) is commercially available. This molecule, initially non-fluorescent, is able to release fluorescein, a highly fluorescent compound, upon interaction with ROS.<sup>8,12</sup> In an earlier publication, we investigated the mechanism of reaction of the HPF sensor.<sup>12</sup> We demonstrated the ability of HPF to react with peroxy radicals and other oxidizing agents. We also characterized the formation of the corresponding phenoxyl radical as the initial oxidation product and we proposed that the reaction was then followed by radical–radical reactions and hydrolysis, the latter being responsible for the release of the fluorescent moiety.

The key characteristic of fluorescent sensors of this type is the covalent binding between a fluorescent moiety and a removable fluorescence quencher. In the case of HPF, these functions are performed by moieties derived from fluorescein and *p*-hydroxyquinone, respectively.

In the present work, we have used a similar concept for the design of a new fluorescent sensor for ROS. We synthesized a new molecule, NBFhd, which contains a fluorescent compound, *N*-methyl-4-amino-7-nitrobenzofurazan (NBF), tethered to a phenolic structure that acts as a quencher and also as a hydrogen donor. This new sensor has several key advantages over HPF, including a simple high-yield and inexpensive synthesis, an exceptionally high

contrast, and fluorescence in a region of the visible spectrum that minimizes interference by cell autofluorescence.

## Experimental

### Synthesis of nitrobenzofurazan derivatives

All the chemicals were purchased from Aldrich and used as received. The <sup>1</sup>H and <sup>13</sup>C NMR spectra were recorded on a Bruker-Avance-400 spectrometer at 400 MHz. Samples were prepared in methyl sulfoxide-*d*<sub>6</sub> (99%) purchased from Aldrich. The chemical shifts are quoted using the  $\delta$  scale and the coupling constants are expressed in Hz. Mass spectra (EI) were recorded on a Kratos-Concept-II instrument.

#### 1. Synthesis of *N*-methyl-4-amino-7-nitrobenzofurazan (NBF).

The compound NBF was prepared according to the literature procedure.<sup>13</sup> Briefly, 1 g of 4-chloro-7-nitrobenzofurazan (5 mmol) was dissolved in 30 ml of methanol, to which 7.5 mmol of methylamine hydrochloride was added. The mixture was refluxed at 75 °C under N<sub>2</sub>. Then 1.26 g (15 mmol) of sodium hydrogen carbonate, dissolved in 20 ml of millipore water, was added dropwise while stirring. While cooling, red crystals of the desired compound precipitated. <sup>1</sup>H NMR (DMSO-*d*<sub>6</sub>, 298 K):  $\delta$  = 3.05 (s, 3H), 6.3 (d, *J* = 8.8 Hz, 1H), 8.51 (d, *J* = 8.8 Hz, 1H), 9.48 (s, 1H). <sup>13</sup>C NMR (DMSO-*d*<sub>6</sub>, 298 K, decoupled):  $\delta$  = 30.59, 99.5, 121.14, 138.45, 144.49, 144.72, 146.26. Mp: 259 °C–261 °C (264 °C–265 °C).<sup>13</sup> EI found: 194 *m/z*.

#### 2. Synthesis of 4[*N*-methyl-*N*(4-hydroxyphenyl)amino]-7-nitrobenzofurazan (NBFhd).

The synthesis of NBFhd has never been reported previously. 500 mg of 4-chloro-7-nitrobenzofurazan (2.5 mmol) was dissolved in 20 ml of methanol, to which 1.29 g (3.75 mmol) of 4-(methylamino)phenol sulfate was added. The mixture was refluxed at 75 °C under N<sub>2</sub> for 1 h. Then 0.76 g (7.5 mmol) of sodium hydrogen carbonate, dissolved in 10 ml of millipore water, was added dropwise under stirring. While cooling, bright red crystals of the desired compound precipitated (668 mg, 93% yield). <sup>1</sup>H NMR (DMSO-*d*<sub>6</sub>, 298 K):  $\delta$  = 3.81 (s, 3H), 6.21 (d, *J* = 8.8 Hz, 1H), 6.89 (d, *J* = 8.8 Hz, 2H), 7.24 (d, *J* = 8.8 Hz, 2H), 8.45 (d, *J* = 9.2 Hz, 1H), 9.97 (s, 1H). <sup>13</sup>C NMR (DMSO-*d*<sub>6</sub>, 298 K, decoupled):  $\delta$  = 45.2, 104.64, 117.1, 121.58, 127.89,

University of Ottawa, Department of Chemistry, 10 Marie Curie, Ottawa, ON, K1N 6N5, Canada. E-mail: tito@photo.chem.uottawa.ca

† Electronic supplementary information (ESI) available: NMR spectra, crystal structures, ORTEP diagrams, crystallographic data for nitrobenzofurazan derivatives, and color representations of the calculated structures from Fig. 6 and 7. See DOI: 10.1039/b702618h

136.64, 137.32, 145.17, 145.18, 147.04, 157.79. Mp: 250 °C–252 °C. The accurate mass was measured to be 286.0648  $m/z$  for a structure  $C_{13}H_{10}N_4O_4$ . X-ray quality crystals were grown by slow evaporation of a dimethylformamide–dichloromethane solution. The data and the structure of the molecule are shown in the ESI†.

### Fluorescence measurements

Steady state emission spectra were recorded using a Photon Technology International fluorimeter. The excitation of the sensor was set at 468 nm. When necessary, the temperature was maintained at 40 °C using a cuvette holder equipped for circulating thermostated water.

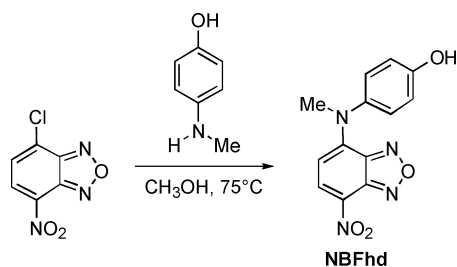
Lifetime fluorescence measurements were performed on a easylife LS (Photon Technology International). The excitation was performed with a 440 nm pulsed LED and the emission was measured at 525 nm.

### Computational details

All calculations were performed using the Gaussian 03 suite of programs.<sup>14</sup> Optimized gas-phase geometries were obtained using the Becke3 exchange functional,<sup>15</sup> in combination with the Lee, Yang, and Parr correlation functional,<sup>16</sup> *i.e.* the B3LYP method, as implemented in Gaussian 03. The 6–31+G(d',p') basis set<sup>17–23</sup> was used for geometry optimizations and energy calculations. Calculating the harmonic vibrational frequencies and noting the number of imaginary frequencies confirmed the nature of all the intermediates (NImag = 0). Solvent effects were approximated with single-point calculations using B3LYP/6–31+G(d',p') on gas-phase B3LYP/6–31+G(d',p') geometries using the IEF-PCM method<sup>24–26</sup> with the water solvent parameters. The atomic radii for the IEF-PCM calculations were specified using the UAHF keyword, while the free energy of solvation was generated using the SCFVAC keyword. Mulliken<sup>27</sup> atomic spin densities were obtained from the gas-phase B3LYP/6–31+G(d',p') geometries.

## Results and discussion

Our main interest was to develop a sensor able to release a molecule with a fluorescence maximum in a region where cellular fluorochromes such as flavin and NADPH do not show a significant autofluorescence.<sup>28</sup> *N*-methyl-4-amino-7-nitrobenzofurazan (NBF) proved to be an interesting candidate.<sup>13,29–31</sup> This molecule presents an absorption maximum at 468 nm and a fluorescence maximum at 540 nm, well separated from cell autofluorescence. The synthesis of NBFhd was based on a strategy similar to that reported by Heberer *et al.*<sup>13</sup> The high-yield one-pot synthesis is outlined in Scheme 1.



Scheme 1 Synthesis of NBFhd.

The structure of NBFhd was unequivocally determined by X-ray crystallography on a crystal obtained from a mixture of dimethylformamide and dichloromethane (see ESI†). The accurate mass of NBFhd gave 286.0648  $g\ mol^{-1}$  and is in agreement with the proposed structure.  $^1H$  and  $^{13}C$  NMR spectra of NBFhd are also consistent with the proposed structure and confirm the purity of the sample (see ESI†).

The new probe, NBFhd, presents an absorption maximum at 500 nm (Fig. 1) with a molar extinction coefficient of 22810  $M^{-1}\ cm^{-1}$ ; NBFhd does not show any fluorescence within our detection limit, thus offering excellent contrast for the detection of ROS. The absence of fluorescence can be rationalized on the basis of an electron transfer between the phenol moiety and the excited NBF chromophore. Indeed, as reported on the Stern–Volmer plot in Fig. 2, phenol is able to quench the fluorescence of excited NBF. The fluorescence lifetime of NBF was measured as 6.0 ns (data not shown), which gives a measured quenching constant of  $3.6 \times 10^{10}\ M^{-1}\ s^{-1}$ . This value is diffusion controlled, which is not surprising since a similar value has already been reported for fluorescence quenching of eosin by phenol.<sup>32</sup> In phosphate buffer at pH 7 containing 1% DMSO, the two molecules, NBF and NBFhd, obey the Beer–Lambert law between at least  $1 \times 10^{-7}\ M$  and  $5 \times 10^{-5}\ M$ , indicating the absence of self-association in the ground state.

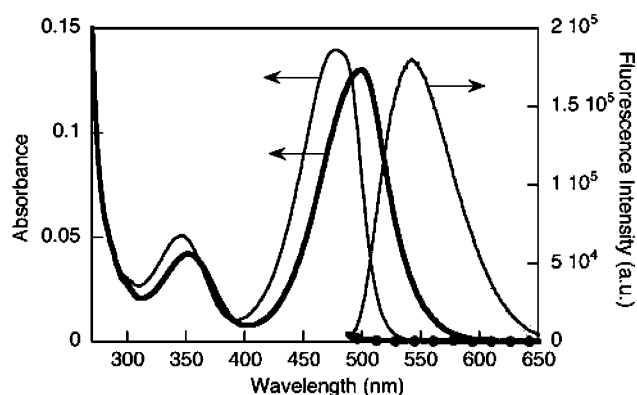


Fig. 1 Absorption (left) and fluorescence (right) spectra of a  $5 \times 10^{-6}\ M$  solution of NBF (thin line) and NBFhd (thick line) in phosphate buffer solution (PBS) at pH 7.4. The excitation wavelength was set at 468 nm and fluorescence spectra (right axis) for unexposed samples include a few identifier points (●).

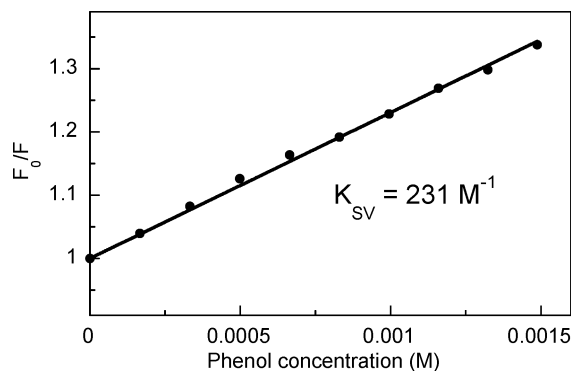
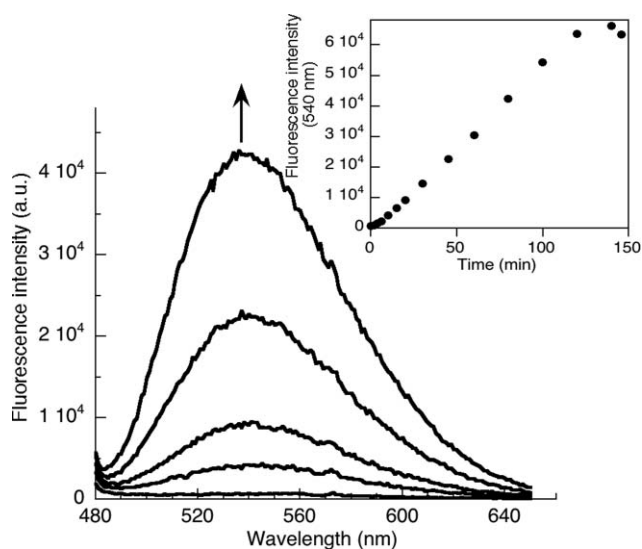


Fig. 2 Stern–Volmer plot of the quenching of fluorescence of a  $5 \times 10^{-6}\ M$  NBF solution in methanol by phenol.

The ability of the new fluorescent probe, NBFhd, to react with reactive oxygen species was monitored by fluorescence spectroscopy. As illustrated in Fig. 3, when peroxy radicals are generated by the thermal decomposition of 2,2'-azobis(2-amidinopropane) dihydrochloride (AAPH) at 40 °C in aerated solutions,<sup>33,34</sup> an increase in fluorescence is observed with time and was attributed to the release of the fluorescent NBF molecule following radical attack on NBFhd; this was demonstrated by HPLC with fluorescence detection (see ESI†). The decrease of fluorescence observed in Fig. 3 after 120 min is likely due to peroxy radical attack on NBF.



**Fig. 3** Evolution of the fluorescence intensity of an aerated NBFhd ( $5 \times 10^{-6}$  M) solution in PBS (pH 7.4) at 40 °C in the presence of AAPH ( $5 \times 10^{-3}$  M). The excitation wavelength was set at 468 nm. The inset represents the evolution of the intensity at 540 nm.

The increase of fluorescence shown in Fig. 3 is completely inhibited when TROLOX (a water soluble analog of Vitamin E and an excellent hydrogen donor) is present in solution (Fig. 4), indicating that the release of NBF from NBFhd is due to its reaction with peroxy radicals. The fact that an equimolar

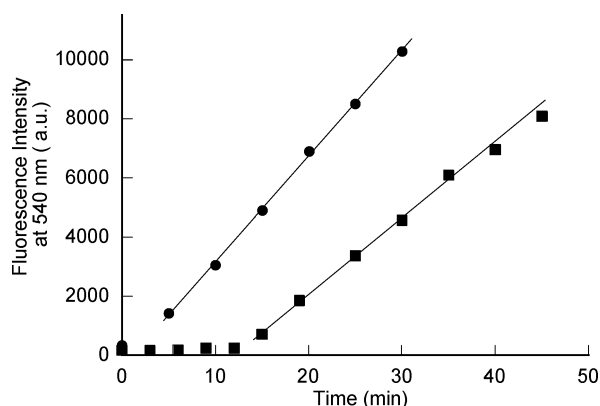
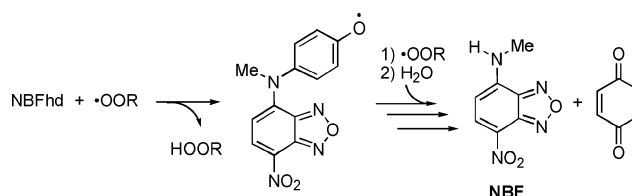


**Fig. 4** Effect of the addition of TROLOX,  $5 \times 10^{-6}$  M, on the release of NBF from a NBFhd solution ( $5 \times 10^{-6}$  M) in PBS (pH 7.4) at 40 °C in presence of AAPH  $5 \times 10^{-3}$  M. Circles correspond to the solution in the absence of TROLOX and the squares are the solution in presence of TROLOX. The wavelength of excitation was set at 468 nm.

concentration of TROLOX totally suppresses the release of NBF suggests that the rate constant for radical attack on TROLOX is significantly faster than that for NBFhd.

A GC/MS analysis of the products of the reaction between NBFhd and peroxy radicals indicate that 1,4-benzoquinone is a product formed in this reaction (see ESI†). The results suggest that the mechanism of reaction of the NBFhd sensor is similar to that proposed for the commercially available probe, HPF.<sup>12</sup> Peroxy radicals are expected to abstract the hydrogen atom from the phenolic moiety leading to the formation of the corresponding phenoxyl radical, followed by reaction with a second peroxy radical and water as shown in Scheme 2. In aqueous solution hydrogen atom transfer is likely mediated by electron transfer.<sup>35,36</sup>



**Scheme 2** Proposed mechanism of reaction of the NBFhd sensor with peroxy radicals.

Density functional theory (DFT) calculations at the B3LYP/6-31+G(d',p') level of theory indicate that hydrogen abstraction from NBFhd by the model peroxy radical  $\cdot\text{OOCH}_3$  is approximately thermoneutral (Fig. 5).

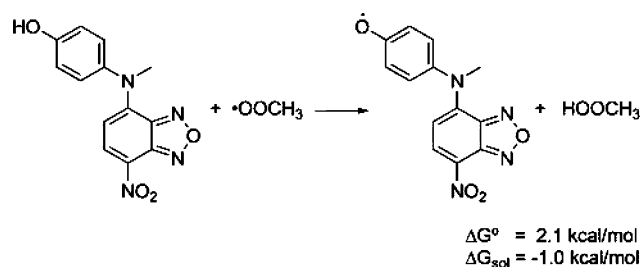


**Fig. 5** Calculated gas-phase and solvent corrected relative free energy of hydrogen abstraction.

Analysis of the spin density of the NBFhd radical reveals that the radical character is delocalized throughout the phenol moiety, with the greatest spin densities located on the phenol oxygen and on the carbon atoms that are *ortho* and *para* to the phenol oxygen (Fig. 6), as expected.

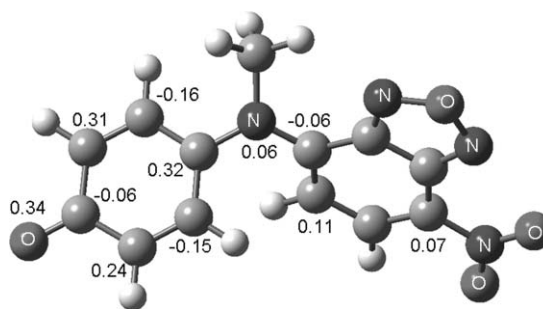


**Fig. 6** Mulliken atomic spin densities of the NBFhd radical at the B3LYP/6-31+G(d',p') level of theory. Spin densities between  $-0.05$  and  $0.05$  are not shown. Unlabeled atoms are C (grey) and H (light grey).

It is believed that the mechanism by which a second peroxy radical and water react with the NBFhd radical to release NBF and 1,4-benzoquinone involves attack at the *para*-position. However, regardless of the mechanism by which NBF is released, the NBFhd radical that was generated by hydrogen transfer, likely will couple with other radicals, including peroxy radicals. Using a smaller model (Model 2, Fig. 7), we calculated the structures and energies of isomers in which the peroxy radical coupled to the NBFhd radical in the *ortho*- and *para*-positions. These calculations revealed that all of the conformers in which coupling occurs at the *ortho*-positions are lower in energy than the isomers in the *para*-position, which is likely because of the steric bulk of the NBF unit.

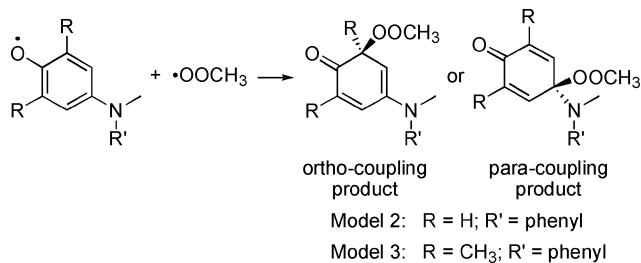


**Fig. 7** Gas-phase relative free energies of the *ortho*- and *para*-coupling products for two models at the B3LYP/6-31+G(d,p) level of theory compared to the gas-phase relative free energy of  $\cdot\text{OC}_6\text{R}_2\text{H}_2\text{NCH}_3\text{R}' + \cdot\text{OOCH}_3$  set to 0.0 kcal mol<sup>-1</sup> (see ESI† for structures and computational details).

The favorable energetics for formation of the *ortho*-coupling product may serve as a side reaction that does not involve NBF release. This result might explain why experimentally only 15 to 20% of NBF is released from the reaction of NBFhd with the peroxy radical.

The interaction of NBFhd with other reactive oxygen species (ROS) was also investigated. As shown in Fig. 8, NBFhd is able to react with  $\cdot\text{OH}$  and  $\text{O}_2^{\cdot-}$  to release NBF, while  $\text{H}_2\text{O}_2$  seems to have no effect on the fluorescent sensor. We note that only qualitative comparisons can be made from these results since the rate of production of ROS, as well as the rate constant of NBFhd towards those ROS, are not known.

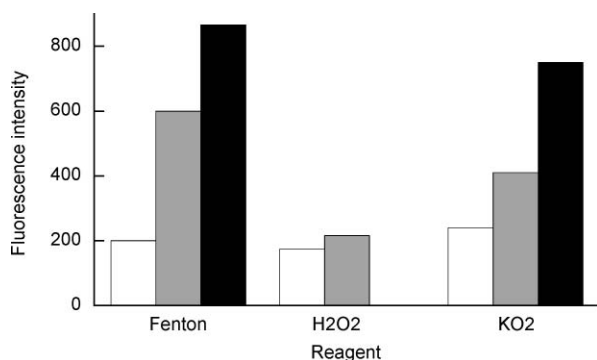


**Fig. 8** Fluorescence increase from a  $5 \times 10^{-6}$  M solution in PBS pH 7.4 upon reaction with  $\cdot\text{OH}$  produced by a Fenton reaction [ $\text{H}_2\text{O}_2$  1 mM (white block), after addition of  $\text{FeSO}_4$  100  $\mu\text{M}$  (grey block), after a second addition of  $\text{FeSO}_4$  100  $\mu\text{M}$  (black box)],  $\text{H}_2\text{O}_2$  100  $\mu\text{M}$  at 40 °C (white block  $t = 0$  min, grey block  $t = 30$  min) and  $\text{O}_2^{\cdot-}$  produced by decomposition of  $\text{KO}_2$  100  $\mu\text{M}$  at 40 °C (white block  $t = 0$  min, grey block  $t = 30$  min, black block  $t = 60$  min).

While the NBF released shows fluorescence emission in a region where cell autofluorescence is weak, its fluorescence quantum yield is modest in water (0.026<sup>31</sup>). However, according to Uchiyama *et al.*,<sup>31</sup> the fluorescence quantum yield increases when the polarity of the solvent decreases; this quantum yield was estimated to be 0.23 in methanol, 0.31 in ethanol and 0.37 in propanol. The polarity of those solvents is close to that found within membranes.<sup>37</sup> The polarity of NBF and NBFhd is also such that its partition in biological media will favor phases with intermediate polarity, rather than the aqueous phase. Therefore, we can expect an increase of the NBF fluorescence quantum yield within membranes and other biomaterials, providing an interesting prospect for the use of this new fluorescent sensor in biological applications.

The new fluorescent sensor, NBFhd, presents several advantages compared to the available HPF probe. Indeed, its inexpensive synthesis required only one step for a yield approaching 100%, while according to the literature, the multistep synthesis of HPF gave only 7% overall yield.<sup>8</sup> In addition, the precursors are readily available, the NBFhd system presents minimal interference with cell autofluorescence and outstanding contrast between unreacted and reacted probe.

We have employed a computational chemistry approach to establish if we could favor the formation of *para*-coupling products by introducing steric bulk in the form of methyl groups at the *ortho*-positions (Model 3, Fig. 6). The relative energies of the isomers of the coupling products for the dimethyl system (Model 3) reveal that coupling to the *ortho*-positions is less favorable as compared to the corresponding products for Model 2. In addition, for the dimethyl complexes, the *ortho*- and *para*-coupling isomers are closer in energy and less favorable energetically, which leads to more *para*-coupling, and as a result may help minimize dead-end pathways.

## Conclusion

In summary, a new fluorescent sensor for reactive oxygen species (ROS) detection has been developed. The initially non-fluorescent NBFhd, a 4,7-disubstituted benzofurazan, reacts with peroxy radicals in phosphate buffer to release a strongly fluorescent compound: NBF. The release of NBF is accompanied by the formation of 1,4-benzoquinone, as demonstrated by chromatographic techniques. NBFhd is a new tool to explore the involvement of reactive oxygen species, in particular oxygen centered radicals, including superoxide, for biological applications.

## Acknowledgements

This work was generously supported by funding from the Natural Sciences and Engineering Research Council of Canada, by the Canadian Foundation for Innovation and by the Government of Ontario. We would like also to thank Dr. Ilia Korobkov for his help with the X-ray experiments.

## References

- 1 R. Colavitti and T. Finkel, *IUBMB Life*, 2006, **57**, 277.
- 2 B. Halliwell and J. M. C. Gutteridge, *Free Radicals in Biology and Medicine*, Oxford University Press, Oxford, U. K., 1989.
- 3 D. Harman, *Age*, 1983, **6**, 86.

- 4 C. Hazelwood and M. J. Davies, *J. Chem. Soc., Perkin Trans. 2*, 1995, **5**, 895.
- 5 C. P. Schulze and R. T. Lee, *Curr. Atheroscler. Rep.*, 2005, **7**, 242.
- 6 G. Waris and H. Ahsan, *J. Carcinog.*, 2006, **5**.
- 7 T. Kalai, E. Hideg, I. Vass and K. Hideg, *Free Radical Biol. Med.*, 1998, **24**, 649.
- 8 K. Setsukinai, Y. Urano, K. Kakinuma, H. J. Majima and T. Nagano, *J. Biol. Chem.*, 2003, **278**, 3170.
- 9 K. Setsukinai, Y. Urano, K. Kikuchi, T. Huguchi and T. Nagano, *J. Chem. Soc., Perkin Trans. 2*, 2000, **12**, 2453.
- 10 T. Ueno, Y. Urano, H. Kojima and T. Nagano, *J. Am. Chem. Soc.*, 2006, **128**, 10640.
- 11 M. Yuasa and K. Oyaizu, *Curr. Org. Chem.*, 2005, **9**, 1685.
- 12 B. Heyne, V. Maurel and J. C. Scaiano, *Org. Biomol. Chem.*, 2006, **4**, 802.
- 13 H. Heberer and H. Kersting, *J. Prakt. Chem.*, 1985, **327**, 487.
- 14 M. J. Frisch, G. W. Trucks, H. B. Schlegel, G. E. Scuseria, M. A. Robb, J. R. Cheeseman, J. J. A. Montgomery, T. Vreven, K. N. Kudin, J. C. Burant, J. M. Millam, S. S. Iyengar, J. Tomasi, V. Barone, B. Mennucci, M. Cossi, G. Scalmani, N. Rega, G. A. Petersson, H. Nakatsuji, M. Hada, M. Ehara, K. Toyota, R. Fukuda, J. Hasegawa, M. Ishida, T. Nakajima, Y. Honda, O. Kitao, H. Nakai, M. Klene, X. Li, J. E. Knox, H. P. Hratchian, J. B. Cross, V. Bakken, C. Adamo, J. Jaramillo, R. Gomperts, R. E. Stratmann, O. Yazyev, A. J. Austin, R. Cammi, C. Pomelli, J. W. Ochterski, P. Y. Ayala, K. Morokuma, G. A. Voth, P. Salvador, J. J. Dannenberg, V. G. Zakrzewski, S. Dapprich, A. D. Daniels, M. C. Strain, O. Farkas, D. K. Malick, A. D. Rabuck, K. Raghavachari, J. B. Foresman, J. V. Ortiz, Q. Cui, A. G. Baboul, S. Clifford, J. Cioslowski, B. B. Stefanov, G. Liu, A. Liashenko, P. Piskorz, I. Komaromi, R. L. Martin, D. J. Fox, T. Keith, M. A. Al-Laham, C. Y. Peng, A. Nanayakkara, M. Challacombe, P. M. W. Gill, B. Johnson, W. Chen, M. W. Wong, C. Gonzalez and J. A. Pople, *Gaussian 03, Revision B.04*, Gaussian, Inc, Wallingford, CT, 2004.
- 15 A. D. Becke, *J. Chem. Phys.*, 1993, 5648.
- 16 C. Lee, W. Yang and R. G. Parr, *Phys. Rev. B*, 1988, **37**, 785.
- 17 T. Clark, J. Chandrasekhar, G. W. Spitznagel and P. Von Ragué Schleyer, *J. Comput. Chem.*, 1983, **4**, 294.
- 18 R. Ditchfield and J. A. Pople, *J. Chem. Phys.*, 1971, **54**, 724.
- 19 J. B. Foresman and M. J. Frisch, *Exploring Chemistry with Electronic Structure Methods*, Gaussian, Inc., Pittsburgh, PA, 2nd edn, 1996.
- 20 P. C. Hariharan and J. A. Pople, *Theor. Chim. Acta*, 1973, **28**, 213.
- 21 W. J. Hehre, R. Ditchfield and J. A. Pople, *J. Chem. Phys.*, 1972, **56**, 2257.
- 22 G. A. Petersson and M. A. Al-Laham, *J. Chem. Phys.*, 1991, **94**, 6081.
- 23 G. A. Petersson, A. Bennett, T. G. Tensfeldt, M. A. Al-Laham, W. A. Shirley and J. Mantzaris, *J. Chem. Phys.*, **89**, 2193.
- 24 E. Cancès, B. Mennucci and J. Tomasi, *J. Chem. Phys.*, 1997, **107**, 3032.
- 25 M. Cossi, V. Barone, B. Mennucci and J. Tomasi, *J. Chem. Phys. Lett.*, 1998, **286**, 253.
- 26 M. Cossi, G. Scalmani, N. Rega and V. Barone, *J. Chem. Phys.*, 2002, **117**, 43.
- 27 R. S. Mulliken, *J. Chem. Phys.*, 1955, **23**, 1833.
- 28 J. E. Aubin, *J. Histochem. Cytochem.*, 1979, **27**, 36.
- 29 A. Buldt and U. Karst, *Anal. Chem.*, 1999, **71**, 3003.
- 30 S. Uchiyama, T. Santa, T. Fukushima, H. Homma and K. Imai, *J. Chem. Soc., Perkin Trans. 2*, 1998, 2165.
- 31 S. Uchiyama, T. Santa and K. Imai, *J. Chem. Soc., Perkin Trans. 2*, 1999, 2525.
- 32 L. I. Grossweiner and E. F. Zwicker, *J. Chem. Phys.*, 1961, **34**, 1411.
- 33 M. A. Cubillos, E. A. Lissi and E. B. Abuin, *Chem. Phys. Lipids*, 2000, **104**, 49.
- 34 G. S. Hammond and R. C. J. Neuman, *J. Am. Chem. Soc.*, 1963, **85**, 1501.
- 35 G. Litwinienko and K. U. Ingold, *J. Org. Chem.*, 2003, **68**, 3433.
- 36 G. Litwinienko and K. U. Ingold, *Acc. Chem. Res.*, 2007, 10.1021/ar0682029.
- 37 W. K. Subczynski, A. Wisniewska, J. J. Yin, J. S. Hyde and A. Kusumi, *Biochemistry*, 1994, **33**, 7670.